INSTITUT FÜR INFORMATIK

The Hilbert Transform on the Two-Sphere: A Spectral Characterization

Oliver Fleischmann

Bericht Nr. 0924
Dezember 2009

CHRISTIAN-ALBRECHTS-UNIVERSITÄT

ZU KIEL

Institut für Informatik der
Christian-Albrechts-Universität zu Kiel
Olshausenstr. 40
D – 24098 Kiel

The Hilbert Transform on the Two-Sphere: A Spectral Characterization

Oliver Fleischmann

Bericht Nr. 0924
Dezember 2009

e-mail: ofl@ks.informatik.uni-kiel.de

Contents

1 Introduction

The Hilbert transform on the real line is a standard tool in one dimensional signal processing. It is the fundamental part of the analytic signal invented by Dennis Gabor [15]. With the *analytic signal* the instantaneous amplitude and phase of a one dimensional signal can be determined. Ever since the analytic signal has been invented, there have been numerous attempts to construct a generalization in higher dimensions. On the one hand the signal and image processing community tried to generalize the analytic signal in order to obtain the instantaneous phase, amplitude and orientation of certain higher dimensional signals [6], [11]. On the other hand the Clifford analysis community proposed several generalizations of the Hilbert transform which arise as boundary values of the Cauchy transform [27], [8], [4], [5]. In image processing the *monogenic signal* introduced in [11], which is a generalization of the analytic signal to two dimensional input signals, is widely used [16], [20], [24], [22]. It is able to determine the instantaneous phase, amplitude and orientation of intrinsically one dimensional signals, that is the real part of a two dimensional plane wave. A further generalization extending the monogenic signal has been derived in [32]. It projects the two dimensional input signal to the unit sphere in $\mathbb{R}^3$ and applies the three dimensional Riesz transform, the analogue of the Hilbert transform in n-dimensional Euclidean space, to obtain the instantaneous phase, amplitude and isophote curvature of the signal. Nonetheless the purpose of both generalizations, the monogenic and the conformal monogenic signal, is to analyze signals defined in the Euclidean plane $\mathbb{R}^2$. Scientific disciplines like geophysics, astrophysics and computer vision have to deal with input signals which are naturally defined on the unit sphere. These signals are for instance seismic or gravitational data captured around the earth [7], satellite data [14], cosmic microwave background [19] or omnidirectional images captured by a catadioptric camera [3], [18]. One seeks for local operators acting on functions naturally defined on the sphere for feature detection. Classical low-level feature detectors are based on derivatives. Since derivatives act as high pass filters they are embedded in a scale space framework, traditionally the Gaussian scale space, to select certain frequency bands. The Hilbert and Riesz transform in the Euclidean space can be thought of as derivative filters without the high pass characteristic, therefore only acting on angular portions of a given function. This property justifies them as useful operators for phase based feature analysis and enables an illumination and rotation invariant detection of low-level features including edges and corners. If we switch to the sphere instead of the Euclidean plane and work in a spherical coordinate system, we would like to be able to use derivatives with respect the azimuthal and longitudal angles. Furthermore we want to use a local derivative-like operator, according to the Riesz transform in the plane. Therefore we seek for an analogue of the Riesz transform in the plane on the sphere.

We will construct a generalization of the analytic signal on the unit sphere $\mathbb{S}^2$ with the help of the Hilbert and the Cauchy transform on $\mathbb{S}^2$. We proceed as follows: In Section 2 we introduce the mathematic preliminaries for our analysis on $\mathbb{S}^2$ to keep this paper self contained. In section 4 we identify the Cauchy transform as our new generalization of the Hilbert transform in a Poisson scale space concept. We derive and discuss the filter kernels for our new signal model and give an important characterization in the spherical harmonic domain in terms of their spherical harmonic coefficients. While the scalar zonal Poisson or Abel-Poisson kernel is a standard tool in multiscale and texture analysis on $\mathbb{S}^2$ and $SO(3)$ (see e.g. [13], [25], [26], [2]), we investigate its harmonic conjugate function arising in the Clifford algebra embedding. The key to the spherical harmonic expansion is the identification of the Cauchy transform on $\mathbb{S}^2$ with a directional correlation introduced in [31]. With the spectral characterization and the resulting interpretation we demonstrate the obtained scale space in Section 5 and analyze the results of the obtained kernels acting on the real part of a plane wave in $\mathbb{R}^3$ restricted to the sphere.

2 Preliminaries

Throughout this paper we work in the universal *Clifford algebra* $\mathbb{R}_{0,n}$ over the vector space $\mathbb{R}^{0,n}$ which is the real vector space $\mathbb{R}^n$ equipped with a non-degenerate quadratic signature $(0,n)$. For an orthonormal basis $(e_1,...,e_n)$ of $\mathbb{R}^{0,n}$ the following multiplication rules arise in $\mathbb{R}_{0,n}$:

$$e_ie_j + e_je_i = -2\delta_{ij}, \quad \forall i,j \in \{1,..,n\} \tag{2.1}$$

In the following the notation $e_ie_j = e_{ij}$ is used. Now for sets $A = \{i_1,...,i_h\} \subseteq \{1,...,n\}$ with $1 \leq i_1 \leq ... \leq i_h \leq n$ and $e_A = e_{i_1}e_{i_2}...e_{i_h}$ the basis $(e_A : A \subseteq \{1...n\})$ forms a basis for the Clifford algebra $\mathbb{R}_{0,n}$. Therefore an element $a \in \mathbb{R}_{0,n}$ allows the representation $a = \sum_{k=0}^{n}[a]_k$ where $[a]_k = \sum_{|A|=k} a_Ae_A$ is called *k-vector*. Vectors $x = (x_1,...,x_n) \in \mathbb{R}^n$ are identified with one-vectors $x = \sum_{j=1}^{n} x_je_j$. The product of two vectors $x,y \in \mathbb{R}_{0,n}$ is then defined by

$$xy = -\langle x,y\rangle + x \wedge y \tag{2.2}$$

where the *inner product*

$$x \bullet y = \langle x,y\rangle = \sum_{i=1}^{n} x_iy_i = -\frac{1}{2}(xy + yx) \tag{2.3}$$

results in a scalar and the *wedge product* or *outer product*

$$x \wedge y = \sum_{i<j} e_ie_j(x_iy_j - x_jy_i) = -\frac{1}{2}(xy + yx). \tag{2.4}$$

results in a two-vector which is also known as a bivector. The conjugation in $\mathbb{R}_{0,n}$ is given by $\overline{e_i} = -e_i$ and therefore the conjugation of a vector x results in $\overline{x} = -x$.
In the following $\mathbb{S}^2$ denotes the unit sphere in $\mathbb{R}^3$ and $\mathbb{B}^2$ the unit ball respectively. ξ, ω, will be elements of $\mathbb{S}^2$ described by the angles (θ, ϕ) and (α, β) where θ, α are zenithal angles and φ, β are azimuthal angles. In Cartesian coordinates they are written as $\xi = [\sin\theta\cos\varphi, \sin\theta\sin\varphi, \cos\theta]^T$ and $\omega = [\sin\alpha\cos\beta, \sin\alpha\sin\beta, \cos\alpha]^T$. Elements in $\mathbb{B}^2$ are denoted by x, y with $x = r\xi$, $y = r\omega$ and $0 < r < 1$ such that $x = [r\sin\theta\cos\varphi, r\sin\theta\sin\varphi, r\cos\theta]^T$ and $y = [r\sin\alpha\cos\beta, r\sin\alpha\sin\beta, r\cos\alpha]^T$. We identify the north pole η with $[0,0,1]^T$. Furthermore dS will denote the surface measure on $\mathbb{S}^2$ and A_3 denotes the surface area of $\mathbb{S}^2$.
In order to expand a function in $L^2(\mathbb{S}^2)$ into a series we introduce an orthonormal basis for functions in $L^2(\mathbb{S}^2)$.

2.1 Spherical Harmonics

The standard *spherical harmonics* are defined as

$$Y_{l,m}(\theta,\varphi) = \left[\frac{2l+1}{4\pi}\frac{(l-m)!}{(l+m)!}\right]^{1/2} P_l^m(\cos\theta)e^{im\varphi} \tag{2.5}$$

where $P_l^m(x)$ are the *associated Legendre functions*

$$P_l^{(m)}(x) = (-1)^m \, (1-x^2)^{m/2} \, \frac{d^m}{dx^m}\left(P_l(x)\right) \tag{2.6}$$

and $P_l(x)$ are the *Legendre polynomials* given by the Rodrigues' formula

$$P_l(x) = \frac{1}{2^l l!}\frac{d^l}{dx^l}\left[(x^2-1)^l\right]. \tag{2.7}$$

The spherical harmonics form an orthonormal basis for the functions in $L^2(\mathbb{S}^2)$. Every function $f \in L^2(\mathbb{S}^2)$ can be expanded into a *Fourier series* as

$$f(\omega) = \sum_{l\in\mathbb{N}} \sum_{m=-l}^{l} \hat{f}_{l,m} Y_{l,m}(\theta,\varphi) \tag{2.8}$$

where the *Fourier coefficients* $\hat{f}_{l,m}$ are obtained as

$$\hat{f}_{l,m} = \int_0^{2\pi}\int_0^{\pi} f(\theta,\varphi)\overline{Y_{l,m}(\theta,\varphi)}\sin\theta d\theta d\varphi \tag{2.9}$$

We will call the index l the *frequency* of a spherical harmonic and the index m the order respectively.
In the Euclidean plane the convolution operation is based on the multiplication of a translated filter kernel with the target function. On the sphere a translation corresponds to a rotation described by two angles. To expand convolution operations on the sphere into a series, we need an orthonormal basis for rotations which are representations of the group $SO(3)$.

2.2 Wigner-D Functions

According to the spherical harmonics, the *Wigner-D functions*

$$D^l_{m,n}(\rho) = D^l_{m,n}(\theta,\varphi,\psi) = e^{-im\psi} d^l_{m,n}(\cos\theta)e^{-in\varphi} \tag{2.10}$$

form an orthonormal basis for $L^2(SO(3))$ with respect to standard Haar measure. Hence the Fourier series expansion of a function $f \in L^2(SO(3))$ with $\rho \in SO(3)$ reads

$$f(\rho) = \sum_{l\in\mathbb{N}} \frac{2l+1}{8\pi^2} \sum_{m=-l}^{l}\sum_{n=-l}^{l} \hat{f}^l_{m,n}\overline{D^l_{m,n}(\rho)} \tag{2.11}$$

3 Hilbert transform in $\mathbb{R}^n$

The classical Hilbert transform on the real line for functions $f \in L^2(\mathbb{R})$ given by the convolution with the Hilbert kernel

$$\mathcal{H}[f](x) = (f * \frac{1}{\pi})(x) = \frac{1}{\pi} P.V. \int\limits_{\mathbb{R}} \frac{f(y)}{x-y} dy \tag{3.1}$$

has a well known interpretation in the Fourier domain:

$$\mathcal{F}[\mathcal{H}[f]](u) = -i\, sgn(u)\, \mathcal{F}[f](u). \tag{3.2}$$

It therefore justifies the interpretation as a $\frac{\pi}{2}$ phase shift for negative frequencies and a $\frac{-\pi}{2}$ phase shift for positive frequencies. Assuming a sinusoid signal model $f(x) = A(x)\cos(\phi(x))$, where $\phi(x)$ denotes the local phase and $A(x)$ the local amplitude of f, its Hilbert transform is obtained as $\mathcal{H}[f](x) = A(x)\sin(\phi(x))$. The sinusoid signal model together with its Hilbert transform constitutes the *analytic signal* [15]

$$f_a(x) = f(x) + i\,\mathcal{H}[f](x) = A(x)e^{i\phi(x)} \tag{3.3}$$

consisting of strictly positive frequencies in the Fourier domain. The analytic signal is a standard tool in signal processing used to obtain the local phase and local amplitude of sinusoid signals. It arises as the non-tangential boundary value of the *Cauchy transform*. The classical Cauchy integral formula is well known from complex analysis. Its generalization in the sense of Clifford analysis working in the real Clifford algebra $\mathbb{R}_{0,n}$ is given by [9]

Definition 3.0.1 (Cauchy transform in $\mathbb{R}^n$ [8])**.** Let $G \subseteq \mathbb{R}^n$ with smooth boundary $\partial G, x \in G$ and $f \in L^2(\partial G)$. Then the Cauchy transform of f in $\mathbb{R}^n$ is defined as

$$\mathcal{C}[f](x) = \frac{2}{A_n} \int\limits_{\partial G} E(x-y)n(y)f(y)dS(y) \tag{3.4}$$

$$= \frac{2}{A_n} \int\limits_{\partial G} \frac{x-y}{|x-y|^{(n+1)/2}} n(y)f(y)dS(y) \tag{3.5}$$

with dS as the surface element of ∂G, A_n the surface area of ∂G and $n(y)$ the outward pointing unit normal at y. The Cauchy transform generates a *monogenic* function in Gwhich solves the differential equation $\partial\mathcal{C}[f](x) = 0$, where ∂ is the *Dirac operator*. Additionally the Cauchy transform splits into the Poisson transform and conjugate Poisson transform of f [5]:

$$\mathcal{C}[f](x) = \frac{1}{2}\mathcal{P}[f](x) + \frac{1}{2}\mathcal{Q}[f](x) \tag{3.6}$$

$$= \frac{1}{2A_3}\int\limits_{\mathbb{S}^2} \frac{1-|x|^2}{|x-\omega|^3} f(\omega)dS(\omega) \tag{3.7}$$

$$+ \frac{1}{2A_3}\int\limits_{\mathbb{S}^2} \frac{1+|x|^2+2x\omega}{|x-\omega|^3} f(\omega)dS(\omega) \tag{3.8}$$

with non-tangential boundaries values of $\mathcal{P}[f](x)$ and $\mathcal{Q}[f](x)$ given by

$$\lim_{n.t.\, x\to\xi} \mathcal{P}[f](x) = f(\xi), \quad \lim_{n.t.\, x\to\xi} \mathcal{Q}[f](x) = \mathcal{H}[f](\xi). \tag{3.9}$$

We can therefore define *monogenic signals* for any closed subset $G \subseteq \mathbb{R}^n$ with smooth boundary in $\mathbb{R}^n$ as the non-tangential boundary value of the Cauchy transform on that surface. Furthermore the Cauchy transform provides a natural embedding in a *scale-space* concept, the *Poisson scale space*. To emphasize the relationship between the Cauchy transform and the analytic and monogenic signal representations we give some examples:

Example 3.0.2 ($G = \mathbb{R}^2_+, \partial G = \mathbb{R}$)**.** In this case we obtained the classical analytic signal on the real line [15] with $x = (x_0, x_1), x_0 > 0$:

$$\lim_{n.t.\, x\to(0,x_1)} \mathcal{C}[f](x) = f(x) + i\mathcal{H}[f](x) = f_a(x). \tag{3.10}$$

Example 3.0.3 ($G = \mathbb{R}^3_+, \partial G = \mathbb{R}^2$)**.** This case represents the *monogenic signal* [11] with $x = (x_0, \underline{x}) = (x_0, x_1, x_2), x_0 > 0$ and the classical Riesz transforms (see e.g. [29]) R_{x_i}:

$$\lim_{n.t.\, x\to(0,\underline{x})} \mathcal{C}[f](x) = f(x) + R_{x_1}[f](x)e_1 + R_{x_2}[f](x)e_2 = f_m(x). \tag{3.11}$$

4 Hilbert transform on the sphere

We have seen that the Cauchy transform is well defined for subsets $G \subseteq \mathbb{R}^n$ with smooth boundary ∂G. The unit sphere $\mathbb{S}^2$ in $\mathbb{R}^3$ is one of these surfaces and therefore allows the construction of a monogenic signal with the help of the Cauchy transform.
In the following we consider functions $f \in L^2(\mathbb{S}^2)$. We call such functions *signals*, which are band-limited such that there exists a maximum frequency $L \in \mathbb{N}$ with $\hat{f}_{l,m} = 0$ for $l \geq L$. In order to construct an analogue to the analytic and monogenic signal on $\mathbb{S}^2$, we proceed in accordance to (3.6). Using the Cauchy transform on $\mathbb{S}^2$ we obtain a splitting into the Poisson and the conjugate Poisson transform, which is the natural embedding of a monogenic signal on $\mathbb{S}^2$ in the Poisson scale-space. Taking the non-tangential boundary values of the Cauchy transform and therefore of the Poisson and conjugate Poisson transform, we obtain the original function f and its Hilbert transform $\mathcal{H}[f]$ on $\mathbb{S}^2$.

Definition 4.0.4 (Cauchy transform on $\mathbb{S}^2$ [8])**.** Let $x \in \mathbb{B}^2 \setminus \mathbb{S}^2$ with $x = r\xi, \xi \in \mathbb{S}^2, 0 < r < 1$ and $f \in L^2(\mathbb{S}^2)$. Then the Cauchy transform of f on $\mathbb{S}^2$ is defined as

$$\mathcal{C}[f](x) = \frac{2}{A_3} \int\limits_{\mathbb{S}^2} E(x-\omega)\omega f(\omega) dS(\omega) \tag{4.1}$$

$$= \frac{2}{A_3} \int\limits_{\mathbb{S}^2} \frac{x-\omega}{|x-\omega|^3} \omega f(\omega) dS(\omega) \tag{4.2}$$

where $E(x-\omega)$ is the Cauchy kernel on $\mathbb{S}^2$.

In our analysis we want to able to select certain frequency bands in the spectral spherical harmonic domain. Therefore we consider lowpass filtered versions of our signal in a linear scale space in $\mathbb{B}^2$. Given two lowpass filters we construct a bandpass filter as the difference of the two lowpass filters. In the case of the monogenic signal the scale space concept which arises naturally is the Poisson scale space in the upper half space $\mathbb{R}^3_+$ [12]. Analogously the scale space in this context is the Poisson scale space in $\mathbb{B}^2$ which arises naturally from the definition of the Hilbert transform being the non tangential boundary value of the Cauchy transform [9]. Therefore the Cauchy transform encompasses the Hilbert transform in the light of the Poisson scale space in the unit ball. The parameter r acts as the scale parameter. The more r tends towards the origin the more *blurred* or *smoothed* versions of the original signal are obtained. As r moves towards 1 the original signal and its Hilbert transform are obtained. This leads to the following definition of a Hilbert transform on $\mathbb{S}^2$:

Definition 4.0.5 (Hilbert transform on $\mathbb{S}^2$ [8])**.** Let $\xi \in \mathbb{S}^2$ and $f \in L^2(\mathbb{S}^2)$. Then the Hilbert transform of f on $\mathbb{S}^2$ is defined as the Cauchy Principal Value integral

$$\mathcal{H}[f](\xi) = \frac{2}{A_3} P.V. \int_{\mathbb{S}^2} \frac{\xi - \omega}{|\xi - \omega|^3} \omega f(\omega) dS(\omega). \tag{4.3}$$

Due to (3.6) we can analyze the Cauchy transform in two steps by analyzing the Poisson and the conjugate Poisson transform separately. Since the Cauchy transform generates a monogenic function, its component functions are harmonic in $\mathbb{S}^2$ with

$$\Delta \mathcal{P}[f](x) = 0, \quad \Delta \mathcal{Q}[f](x) = 0 \tag{4.4}$$

where Δ is the Laplace operator in $\mathbb{B}^2$.

4.1 The Cauchy transform on $\mathbb{S}^2$ as a directional correlation

It is desirable from a signal processing viewpoint to interpret the Cauchy transform as a filtering operation. In $\mathbb{R}^3$ linear filters are applied to signals by convolution. The convolution on the sphere is the integration over the group $SO(3)$ of the input signal and the filter, as proposed for example by [10]. Since the Cauchy transform integrates over $\mathbb{S}^2$ it can not immediately be identified with a spherical convolution operation. Nonetheless there exists an operation called *directional correlation* introduced in [31]:

Definition 4.1.1 (Directional correlation)**.** Let $\rho \in SO(3)$, $\mathcal{R}(\rho)$ the rotation operator associated with ρ and $h \in L^2(\mathbb{S}^2), f \in L^2(\mathbb{S}^2)$. The directional correlation of h and f in the direction ρ is given by

$$\mathcal{R}(\rho)[h] \star f = \int_{\mathbb{S}^2} \overline{h(\mathcal{R}^{-1}(\rho)\, \omega)} f(\omega) dS(w). \tag{4.5}$$

The directional correlation turns out to be a function in $L^2(SO(3))$. We want to analyze signals on the sphere *locally*. Therefore we are not interested in the global Cauchy transform of a certain signal. Instead every time we evaluate the Cauchy transform at some point on the sphere, we treat this point as the *north pole* η of a sphere, rotated to the evaluation point. The spherical coordinates (θ, φ) at which we evaluate the Cauchy transform describe a rotation $\rho = (\theta, \varphi, 0)$. So with respect to original coordinate system we always evaluate the Cauchy transform at the north pole of a sphere in a *rotated* coordinate system. In that sense we obtain a local analysis of our signal for every point. Furthermore this is the key to the expression of the Cauchy transform as a directional correlation. Suppose we want to evaluate the Cauchy transform at some fixed point $x = r\xi$. Now we choose this point x as the north pole η of some *rotated* coordinate system. Then the Cauchy kernel $E(x - \omega)$ is just a rotated version of the kernel $E(r\eta-\omega)$ centered at the north pole η. The evaluation of the Cauchy transform at a point $x=r\xi\in\mathbb{B}^2$ with spherical coordinates (r,θ,φ) reduces to the evaluation of the Cauchy transform at η rotated by $\rho=(\theta,\varphi,0)$. Thinking of the Cauchy kernel as a filter mask we always use the same filter mask centered at the north pole, but at *every* point we apply it to a *rotated* version of the original function. So for every point $x=r\xi$ we do not actually evaluate the transform with the kernel $E(r\xi-\omega)$ but we evaluate the transform as

$$\mathcal{C}[f](r,\theta,\varphi)=\int_{\mathbb{S}^2} E(r\eta-\omega)\omega f(\mathcal{R}^{-1}(\theta,\varphi,0)\omega)dS(\omega) \tag{4.6}$$

$$=\mathcal{R}(\theta,\varphi,0)[h]\star f. \tag{4.7}$$

4.2 Fourier series expansion

The next step towards an intuitive interpretation of the Hilbert transform of the sphere is the series expansion of the directional correlation. As we have noticed, the directional correlation is a function in $L^2(SO(3))$. The Cauchy transform has been interpreted as a directional correlation evaluated for rotations corresponding to the Euler angle representations $(\theta,\varphi,0)$. In this case the directional correlation is also known as a standard correlation on $\mathbb{S}^2$ according to [31]. We introduced the Wigner-D functions as an orthonormal basis for $L^2(SO(3))$. As a consequence, the directional correlation admits an expansion into a Fourier series on $SO(3)$ in terms of the Wigner-D basis functions. For a series expansion of the Cauchy transform we are in the need of the series expansion coefficients. It has been shown in [31] that the coefficients of the directional correlation can be evaluated in terms of the spherical harmonic coefficients of the function and the filter respectively as

$$\widehat{[\mathcal{R}[h]\star f]}^{l}_{m,n}=\overline{\hat{h}_{l,n}}\hat{f}_{l,m} \tag{4.8}$$

such that the series expansion of the directional correlation reads

$$\mathcal{R}(\rho)[h]\star f=\sum_{l\in\mathbb{N}}\sum_{m=-l}^{l}\sum_{n=-l}^{l}\widehat{[\mathcal{R}[h]\star f]}^{l}_{m,n}\overline{D^{l}_{m,n}(\rho)}. \tag{4.9}$$

Since we want to provide a spectral characterization of the Poisson and conjugate Poisson filter kernels, we have to expand them into a spherical harmonic series. The directional correlation in terms of the spherical harmonic coefficients is now used to evaluate the Cauchy transform. We seek for the spherical harmonic coefficients of the Cauchy kernel. Since the Cauchy transform splits into the Poisson and conjugate Poisson transform we evaluate the coefficients of the Poisson and conjugate Poisson kernel in (3.7), (3.8) separately. The Poisson kernel belongs to the set of zonal functions which are constant for all $\xi\in\mathbb{S}^2$ with $\langle\omega,\xi\rangle=c, c\in[-1,1]$. The spectral characterization of these zonal functions is obtained by the Funk-Heck theorem:

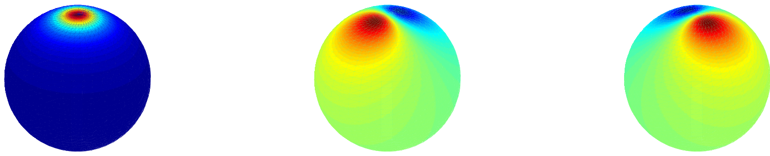

Figure 4.1: From left to right: The Poisson kernel $\mathcal{P}_r$ and the bivector parts of the conjugate Poisson kernel $\mathcal{Q}_r^{(1)}$ and $\mathcal{Q}_r^{(2)}$ for $r = 0.9$.

Theorem 4.2.1 (Funk-Hecke formula on $\mathbb{S}^2$ [13])**.** *Let f be a zonal function on $\mathbb{S}^n$ and $\xi \in \mathbb{S}^n$. Then*

$$\int_{\mathbb{S}^n} f(\langle \xi, \omega \rangle) Y_{l,m}(\omega) dS(\omega) = \lambda_l Y_{l,m}(\xi) \tag{4.10}$$

with the eigenvalue

$$\lambda_l = A_{n-1} \frac{1}{C_l^{(n-1)/2}(1)} \int_{-1}^{1} f(t) C_l^{(n-1)/2}(t)(1-t^2)^{(n-2)/2} dt \tag{4.11}$$

where $C_n^{(n-1)/2}$ is the l-th Gegenbauer polynomial of order $(n-1)/2$. For $n = 2$ the Gegenbauer Polynomials reduce to the Legendre polynomials. In that case the above transform used to obtain the eigenvalues λ_l reduces to the Legendre transform. Using the Funk-Hecke theorem, the zonal Poisson kernel in $\mathbb{B}^2$, also known as the Abel-Poisson kernel, results in the series expansion (see e.g. [13])

$$\mathcal{P}_r(x, \omega) = \frac{1-|x|^2}{|x-\omega|^3} = \frac{1-r^2}{(1-2r\cos\theta + r^2)^{(3/2)}} \sum_{k=0}^{\infty} (2k+1) r^k P_n(\langle \xi, \omega \rangle). \tag{4.12}$$

Remembering that we always evaluate the transforms at the north pole η with $x = x_3 e_3 = r\eta = re_3, 0 < r < 1$ the above series leads to the spherical harmonic coefficients

$$\widehat{[\mathcal{P}_r]}_{l,m} = \int_{\mathbb{S}^2} \mathcal{P}_r(r\eta, \omega) \overline{Y_{l,m}(\omega)} dS(\omega) = \begin{cases} r^l & \text{for } m = 0 \\ 0 & \text{else} \end{cases} \tag{4.13}$$

For the expansion of conjugate Poisson kernel we first rewrite the kernel as

$$\mathcal{Q}_r(x, \omega) = \frac{1+|x|^2 + 2x\omega}{|x-\omega|^3} = \frac{1+|x|^2 - 2r\omega_3}{|x-\omega|^3} - \frac{2r\omega_1 e_{13}}{|x-\omega|^3} - \frac{2r\omega_2 e_{23}}{|x-\omega|^3}. \tag{4.14}$$

with $\omega = [\sin\theta\cos\varphi, \sin\theta\sin\varphi, \cos\theta]^T$ and $x = r\eta$ such that $\langle x, \omega\rangle = \langle r\eta, \omega\rangle = r\cos\theta$. Since $x = r\eta = [0,0,r]^T$ we have

$$|x-\omega|^3 = \left((-\omega_1)^2 + (-\omega_2)^2 + (r-\omega_3)^2\right)^{3/2} = \left(1 + r^2 - 2r\omega_3\right)^{3/2} \tag{4.15}$$

$$= \left(1 + |x|^2 - 2r\omega_3\right)\left(1 + |x|^2 - 2r\omega_3\right)^{1/2} \tag{4.16}$$

such that

$$\frac{1 + |x|^2 - 2r\omega_3}{|x-\omega|^3} = \frac{1}{\left(1 + r^2 - 2r\omega_3\right)^{1/2}}. \tag{4.17}$$

The generating function $\frac{1}{(1+r^2-2r\omega_3)^{1/2}}$ has the series expansion in terms of the Legendre polynomials [17]

$$\frac{1}{\left(1 + r^2 - 2r\omega_3\right)^{1/2}} = \sum_{k=0}^{\infty} r^k P_n(\langle\xi, \omega\rangle) = \sum_{k=0}^{\infty} r^k P_n(\cos\theta). \tag{4.18}$$

Accordingly the generating function $\frac{1}{(1+|x|^2-2r\omega_3)^{3/2}}$ expands into a series of the Gegenbauer polynomials [17]

$$\frac{1}{\left(1 + |x|^2 - 2r\omega_3\right)^{3/2}} = \sum_{k=0}^{\infty} r^k C_n^{3/2}(\langle\xi, \omega\rangle) = \sum_{k=0}^{\infty} r^k C_n^{3/2}(\cos\theta). \tag{4.19}$$

Therefore we obtain a series expansion of the conjugate Poisson kernel in terms of Legendre and Gegenbauer polynomials as

$$\mathcal{Q}_r(x,\omega) = \sum_{k=0}^{\infty} r^k P_n(\cos\theta) \tag{4.20}$$

$$- 2r\omega_1 \sum_{k=0}^{\infty} r^k C_k^{3/2}(\cos\theta) e_{13} - 2r\omega_2 \sum_{k=0}^{\infty} r^k C_k^{3/2}(\cos\theta) e_{23} \tag{4.21}$$

$$= \mathcal{Q}_r^{(0)}(x,\omega) - 2r\mathcal{Q}_r^{(1)}(x,\omega)e_{13} - 2r\mathcal{Q}_r^{(2)}(x,\omega)e_{23} \tag{4.22}$$

While the Poisson kernel only consists of a scalar part, the conjugate Poisson kernel splits into a scalar and two bivector parts. The scalar part of the conjugate Poisson kernel is equal to the ordinary Poisson kernel. Figure 4.1 shows the Poisson kernel and the two bivector parts of the conjugate kernel at a certain scale. We treat the scalar and bivector parts of the conjugate Poisson kernel as three single kernels. For every single kernel the Fourier coefficients are supposed to be determined. In order to obtain the Fourier coefficients of the kernels, we express all parts of the kernels as series depending on the standard spherical harmonics. We introduce the addition theorem for Gegenbauer polynomials with spherical coordinates (r_1, θ, ϕ) and (r_2, α, β), subtended by the angle γ at the origin, as [28]:

$$C_n^\lambda(\cos\gamma) = 4\pi \sum_{m=0}^{\lfloor n/2 \rfloor} \langle\, \mathbf{Y_{n,m}}(\theta,\phi), \overline{\mathbf{Y_{n,m}}(\alpha,\beta)}\,\rangle \tag{4.23}$$

with the vector of scalar spherical harmonics

$$\mathbf{Y_{n,m}}(x,y) = \begin{bmatrix} Y_{l,-l} \\ Y_{l,-l+1} \\ \dots \\ Y_{l,l} \end{bmatrix} \tag{4.24}$$

where $l = n - 2m$ resulting in

$$C_n^\lambda(\cos\gamma) = 4\pi \sum_{m=0}^{\lfloor n/2 \rfloor} \sum_{j=-l}^{l} Y_{l,j}(\theta,\phi)\overline{Y_{l,j}}(\alpha,\beta) \tag{4.25}$$

In addition we expand ω_1 and ω_2 into a Fourier series with the Fourier coefficients

$$\widehat{[\omega_1]}_{l,m} = \int_{\varphi=0}^{2\pi} \int_{\theta=0}^{\pi} \sin\theta\cos\varphi\overline{Y_{l,m}(\theta,\varphi)}d\theta d\varphi = \begin{cases} \pm\sqrt{\frac{2\pi}{3}} & \text{for } m = \mp 1 \\ 0 & \text{else} \end{cases} \tag{4.26}$$

$$\widehat{[\omega_2]}_{l,m} = \int_{\varphi=0}^{2\pi} \int_{\theta=0}^{\pi} \sin\theta\sin\varphi\overline{Y_{l,m}(\theta,\varphi)}d\theta d\varphi = \begin{cases} i\sqrt{\frac{2\pi}{3}} & \text{for } m = \pm 1 \\ 0 & \text{else} \end{cases} \tag{4.27}$$

such that

$$\omega_1 = \sum_{l=0}^{\infty} \sum_{m=-l}^{l} \widehat{[\omega_1]}_{l,m} Y_{l,m}(\theta,\varphi) = \sqrt{\frac{2\pi}{3}} Y_{1,-1}(\theta,\varphi) - \sqrt{\frac{2\pi}{3}} Y_{1,1}(\theta,\varphi) \tag{4.28}$$

$$\omega_2 = \sum_{l=0}^{\infty} \sum_{m=-l}^{l} \widehat{[\omega_1]}_{l,m} Y_{l,m}(\theta,\varphi) = i\sqrt{\frac{2\pi}{3}} Y_{1,-1}(\theta,\varphi) + i\sqrt{\frac{2\pi}{3}} Y_{1,1}(\theta,\varphi). \tag{4.29}$$

We determine the Fourier coefficients of the conjugate Poisson kernel bivector parts as:

$$\widehat{[\mathcal{Q}_r^{(1)}]}_{l,m} = \int_{\mathbb{S}^2} \mathcal{Q}_r^{(1)}(\omega)\overline{Y_{l,m}(\omega)}dS(\omega) \tag{4.30}$$

$$= \int_{\mathbb{S}^2} \omega_1 \sum_{k=0}^{\infty} r^k C_k^{3/2}(\cos\theta)\overline{Y_{l,m}(\omega)}dS(\omega) \tag{4.31}$$

$$\overset{l'=k-2m'}{=} 4\pi \sum_{k=0}^{\infty} r^k \int_{\mathbb{S}^2} \omega_1 \sum_{m'=0}^{\lfloor k/2 \rfloor} \sum_{j=-l'}^{l'} Y_{l',j}(\omega)\overline{Y_{l',j}}(0)\overline{Y_{l,m}(\omega)}dS(\omega) \tag{4.32}$$

$$= 4\pi\sqrt{\frac{2\pi}{3}} \sum_{k=0}^{\infty} r^k \tag{4.33}$$

$$\times \left(\int_{\mathbb{S}^2} Y_{1,-1}(\omega) \sum_{m'=0}^{\lfloor k/2 \rfloor} \sum_{j=-l'}^{l'} Y_{l',j}(\omega)\overline{Y_{l',j}}(0)\overline{Y_{l,m}(\omega)}dS(\omega) \right. \tag{4.34}$$

$$\left. - \int_{\mathbb{S}^2} Y_{1,1}(\omega) \sum_{m'=0}^{\lfloor k/2 \rfloor} \sum_{j=-l'}^{l'} Y_{l',j}(\omega)\overline{Y_{l',j}}(0)\overline{Y_{l,m}(\omega)}dS(\omega) \right) \tag{4.35}$$

$$= 4\pi\sqrt{\frac{2\pi}{3}} \sum_{k=0}^{\infty} r^k \tag{4.36}$$

$$\times \left(\sum_{m'=0}^{\lfloor k/2 \rfloor} \overline{Y_{l',0}}(0) \int_{\mathbb{S}^2} Y_{1,-1}(\omega)Y_{l',0}(\omega)\overline{Y_{l,m}(\omega)}dS(\omega) \right. \tag{4.37}$$

$$\left. - \sum_{m'=0}^{\lfloor k/2 \rfloor} \overline{Y_{l',0}}(0) \int_{\mathbb{S}^2} Y_{1,1}(\omega)Y_{l',0}(\omega)\overline{Y_{l,m}(\omega)}dS(\omega) \right) \tag{4.38}$$

Since $\overline{Y_{l,m}}(\omega) = (-1)^m Y_{l,-m}(\omega)$ the triple integrals evaluate to [30]

$$\int_{\mathbb{S}^2} Y_{1,1}(\omega)Y_{l',0}(\omega)\overline{Y_{l,m}}(\omega)dS(\omega) \tag{4.39}$$

$$= (-1)^m \sqrt{\frac{(2+1)(2l'+1)(2l+1)}{4\pi}} \begin{pmatrix} 1 & l' & l \\ 0 & 0 & 0 \end{pmatrix} \begin{pmatrix} 1 & l' & l \\ 1 & 0 & (-m) \end{pmatrix} \tag{4.40}$$

and

$$\int_{\mathbb{S}^2} Y_{1,-1}(\omega)Y_{l',0}(\omega)\overline{Y_{l,m}}(\omega)dS(\omega) \tag{4.41}$$

$$= (-1)^m \sqrt{\frac{(2+1)(2l'+1)(2l+1)}{4\pi}} \begin{pmatrix} 1 & l' & l \\ 0 & 0 & 0 \end{pmatrix} \begin{pmatrix} 1 & l' & l \\ -1 & 0 & (-m) \end{pmatrix} \tag{4.42}$$

where $\begin{pmatrix} l_1 & l_2 & l_3 \\ m_1 & m_2 & m_3 \end{pmatrix}$ are the *Wigner 3j-symbols*. The Wigner 3j-symbols evaluate to 0 unless they satisfy

$$(i) \quad |l_1 - l_3| \leq l_2 \leq l_1 + l_2 \tag{4.43}$$
$$(ii) \quad m_1 + m_2 = -m_3 \tag{4.44}$$

Therefore it holds that

$$\begin{pmatrix} 1 & l' & l \\ 0 & 0 & 0 \end{pmatrix} = \begin{cases} \begin{pmatrix} 1 & l' & l \\ 0 & 0 & 0 \end{pmatrix} & if \quad l' = l-1 \vee l' = l \vee l' = l+1 \\ \\ 0 & else \end{cases} \tag{4.45}$$

$$\begin{pmatrix} 1 & l' & l \\ \pm 1 & 0 & (-m) \end{pmatrix} = \begin{cases} \begin{pmatrix} 1 & l' & l \\ \pm 1 & 0 & \pm 1 \end{pmatrix} & if \quad m = \mp 1 \\ \\ 0 & else \end{cases} \tag{4.46}$$

Closed expressions for the Wigner 3j-symbols used here are given in [1]:

$$\begin{pmatrix} k & k & 1 \\ q & -q & 0 \end{pmatrix} = (-)^{k-q} \frac{q}{[k(k+1)(2k+1)]^{1/2}} \tag{4.47}$$

$$\begin{pmatrix} k & k+1 & 1 \\ q & -q-1 & 1 \end{pmatrix} = (-)^{k-q} \left[\frac{(k+q+1)(k+q+2)}{2(k+1)(2k+1)(2k+3)} \right]^{1/2} \tag{4.48}$$

$$\begin{pmatrix} k & k+1 & 1 \\ q & -q & 0 \end{pmatrix} = (-)^{k-q} \left[\frac{(k-q-1)(k+q+1)}{(k+1)(2k+1)(2k+3)} \right]^{1/2} \tag{4.49}$$

With (4.47) it follows that that $\begin{pmatrix} 1 & l & l \\ 0 & 0 & 0 \end{pmatrix} = 0$ such that $l' = l-1 \vee l+1$. For $l' = l-1$ we use (4.49) with $k = l-1, q = 0$ and (4.48) with $k = l-1, q = 0$ to obtain

$$(-1)^m Y_{l-1,0}(0) \sqrt{\frac{(2+1)(2(l-1)+1)(2l+1)}{4\pi}} \begin{pmatrix} 1 & l-1 & l \\ 0 & 0 & 0 \end{pmatrix} \begin{pmatrix} 1 & l-1 & l \\ 1 & 0 & -1 \end{pmatrix} \tag{4.50}$$

$$= (-)^{l-1} \sqrt{\frac{2l-1}{4\pi}} \sqrt{\frac{3(2l-1)(2l+1)}{4\pi}} \tag{4.51}$$

$$\times \sqrt{\frac{l^2}{l(2l-1)(2l+1)}} \sqrt{\frac{l(l+1)}{2l(2l-1)(2l+1)}} \tag{4.52}$$

$$= (-)^{l-1} \frac{1}{4\pi} \sqrt{\frac{3l(l+1)}{2(2l+1)}} \tag{4.53}$$

$$(-1)^m Y_{l+1,0}(0)\sqrt{\frac{(2+1)(2(l+1)+1)(2l+1)}{4\pi}}\begin{pmatrix}1 & l+1 & l\\ 0 & 0 & 0\end{pmatrix}\begin{pmatrix}1 & l+1 & l\\ 1 & 0 & -1\end{pmatrix} \tag{4.54}$$

$$= (-)^l\sqrt{\frac{2l+3}{4\pi}}\sqrt{\frac{3(2l+3)(2l+1)}{4\pi}} \tag{4.55}$$

$$\times\sqrt{\frac{(l+1)^2}{(l+1)(2l+1)(2l+3)}}\sqrt{\frac{l(l+1)}{2(l+1)(2l+1)(2l+3)}} \tag{4.56}$$

$$= (-)^l\frac{1}{4\pi}\sqrt{\frac{3l(l+1)}{2(2l+1)}} \tag{4.57}$$

The only contributing terms in the sums are the expressions with $l' = l-1 \vee l+1$. Since $l' = k-2m$, this is only the case for $k = (l-1)+2n, n \geq 0$. For $k = l-1$ this is only true for $n = 0$. For all other k there are always two solutions but as we have seen, they only differ in their sign. Therefore the sum for all $k > l-1$ evaluates to zero such that

$$\widehat{[\mathcal{Q}_r^{(1)}]}_{l,\pm1} = \mp 2r4\pi\sqrt{\frac{2\pi}{3}}\frac{1}{4\pi}\sqrt{\frac{3l(l+1)}{2(2l+1)}}r^{l-1} = \mp\sqrt{\frac{4\pi\, l(l+1)}{(2l+1)}}r^l \tag{4.58}$$

$$\widehat{[\mathcal{Q}_r^{(2)}]}_{l,\pm1} = \mp 2r4\pi\sqrt{\frac{2\pi}{3}}\frac{1}{4\pi}\sqrt{\frac{3l(l+1)}{2(2l+1)}}r^{l-1} = i\sqrt{\frac{4\pi\, l(l+1)}{(2l+1)}}r^l \tag{4.59}$$

The spherical harmonic coefficients characterize the filter kernels in the frequency domain. As one notices the coefficients of the scalar part is zero for $m \neq 0$ whereas the coefficients of the bivector parts are zero for $m \neq \pm1$. The factor r^l indicates the lowpass behaviour of all filter parts since $0 < r < 1$. Using the spherical harmonic coefficients, the Poisson and conjugate Poisson transforms can now be expressed as a directional correlation in the spherical harmonic domain according to (4.9) as

$$\mathcal{R}(\rho)[\mathcal{P}_r]\star f = \sum_{l\in\mathbb{N}}\sum_{m=-l}^{l} r^l \widehat{f}_{l,m}\overline{D^l_{m,0}(\rho)} = \sum_{l\in\mathbb{N}}\sum_{m=-l}^{l} r^l \widehat{f}_{l,m}\overline{Y_{l,m}(\theta,\varphi)} \tag{4.60}$$

$$\mathcal{R}(\rho)[\mathcal{Q}_r^{(1)}]\star f = \sum_{l\in\mathbb{N}}\sum_{m=-l}^{l}\sqrt{\frac{4\pi\, l(l+1)}{(2l+1)}}r^l\widehat{f}_{l,m}\left(\overline{D^l_{m,-1}(\rho)} - \overline{D^l_{m,1}(\rho)}\right) \tag{4.61}$$

$$\mathcal{R}(\rho)[\mathcal{Q}_r^{(2)}]\star f = \sum_{l\in\mathbb{N}}\sum_{m=-l}^{l} i\sqrt{\frac{4\pi\, l(l+1)}{(2l+1)}}r^l\widehat{f}_{l,m}\left(\overline{D^l_{m,-1}(\rho)} + \overline{D^l_{m,1}(\rho)}\right) \tag{4.62}$$

Since we evaluate the correlation for rotations $\rho = (\theta,\varphi,0)$ the Wigner-D functions reduce to *spin-weighted spherical harmonics* [31]

$$ {}_nY_{l,m}(\theta,\varphi) = (-1)^n \sqrt{\frac{2l+1}{4\pi}\overline{D^l_{m,n}(\theta,\varphi,0)}} \tag{4.63} $$

We define the spin raising and lowering operators as [21]

$$ \begin{aligned} \left[\eth\, {}_nG\right](\theta,\phi) &= \left[-\sin^n\theta\left(\tfrac{\partial}{\partial\theta}+\tfrac{i}{\sin\theta}\tfrac{\partial}{\partial\varphi}\right)\sin^{-n}\theta\, {}_nG\right](\theta,\varphi) \\ \left[\overline{\eth}\, {}_nG\right](\theta,\phi) &= \left[-\sin^n\theta\left(\tfrac{\partial}{\partial\theta}-\tfrac{i}{\sin\theta}\tfrac{\partial}{\partial\varphi}\right)\sin^{-n}\theta\, {}_nG\right](\theta,\varphi) \end{aligned} \tag{4.64} $$

With these operators the spin-weighted spherical harmonics are constructed from the scalar spherical harmonics as

$$ \begin{aligned} {}_nY_{l,m}(\theta,\varphi) &= \left[\tfrac{(l-n)!}{(l+n)!}\right]^{1/2}[\eth^n Y_{l,m}](\theta,\varphi) && for \quad 0\le n\le l \\ {}_nY_{l,m}(\theta,\varphi) &= \left[\tfrac{(l-n)!}{(l+n)!}\right]^{1/2}(-1)^n[\overline{\eth^n} Y_{l,m}](\theta,\varphi) && for \quad -l\le n\le 0 \end{aligned} \tag{4.65} $$

With $\rho=(\theta,\varphi,0), \omega=(\theta,\varphi)\in\mathbb{S}^2$ the correlations (4.61), (4.62) reduce to

$$ \mathcal{R}(\rho)[\mathcal{Q}_r^{(1)}]\star f = \sum_{l\in\mathbb{N}}\sum_{m=-l}^{l} r^l \widehat{f}_{l,m}\left({}_{-1}Y_{l,m}(\omega) - {}_1Y_{l,m}(\omega)\right) \tag{4.66} $$

$$ = 2\sum_{l\in\mathbb{N}}\sum_{m=-l}^{l} r^l \widehat{f}_{l,m}\frac{\partial}{\partial\theta}Y_{l,m}(\omega) \tag{4.67} $$

$$ \mathcal{R}(\rho)[\mathcal{Q}_r^{(2)}]\star f = \sum_{l\in\mathbb{N}}\sum_{m=-l}^{l} i\, r^l \widehat{f}_{l,m}\left({}_{-1}Y_{l,m}(\omega) + {}_1Y_{l,m}(\omega)\right) \tag{4.68} $$

$$ = 2\sum_{l\in\mathbb{N}}\sum_{m=-l}^{l} r^l \widehat{f}_{l,m}\frac{1}{\sin\theta}\frac{\partial}{\partial\varphi}Y_{l,m}(\omega) \tag{4.69} $$

The *del* operator in a spherical coordinate system, which coincides with the spherical gradient operator in the case of a scalar valued function, with basis vectors e_r, e_θ, e_φ is defined as

$$ \nabla = e_r\frac{\partial}{\partial r} + e_\theta\frac{1}{r}\frac{\partial}{\partial\theta} + e_\varphi\frac{1}{r\sin\theta}\frac{\partial}{\partial\varphi}. \tag{4.70} $$

It acts on a function $f\in L_2(\mathbb{S}^2)$ as

$$ (\nabla f)(\omega) = \sum_{l\in\mathbb{N}}\sum_{m=-l}^{l} \widehat{f}_{l,m}(\nabla Y_{l,m})(\omega) \tag{4.71} $$

$$ = e_\theta\sum_{l\in\mathbb{N}}\sum_{m=-l}^{l} \widehat{f}_{l,m}\frac{\partial}{\partial\theta}Y_{l,m}(\omega) + e_\varphi\sum_{l\in\mathbb{N}}\sum_{m=-l}^{l} \widehat{f}_{l,m}\frac{1}{\sin\theta}\frac{\partial}{\partial\varphi}Y_{l,m}(\omega). \tag{4.72} $$

Comparing (4.72) with (4.67) and (4.69) one notices that the conjugate Poisson transforms acts like a gradient operator but instead of acting on the original function it acts on the solution of the Laplace equation.

5 Applications

5.1 Poisson scale space

The Poisson transform $\mathcal{P}[f]$ acts as a lowpass filter in the spherical harmonic domain on the frequencies l. Furthermore the Poisson transform generates a harmonic function and solves the Laplace equation in $\mathbb{B}^2$ with boundary values on $\mathbb{S}^2$. It constitutes a linear scale space in $\mathbb{B}^2$ with scale parameter $r = e^{-p}$ for $p \in [0, \infty)$ such that $0 < r < 1$. With this choice for r, for any $p_1, p_2 \in [0, \infty)$ and $f \in L^2(\mathbb{S}^2)$ we have

$$\mathcal{P}_{p_2}[\mathcal{P}_{p_1}[f]] = \sum_{l=0}^{\infty} \sum_{m=-l}^{l} e^{-p1} e^{-p2} \hat{f}_{l,m} Y_{l,m} \tag{5.1}$$

$$= \sum_{l=0}^{\infty} \sum_{m=-l}^{l} e^{-(p1+p2)} \hat{f}_{l,0} Y_{l,m} = \mathcal{P}_{p_1+p_2}[f] \tag{5.2}$$

since we can apply the spherical convolution theorem according to [10] to the convolution with the zonal Poisson kernel. The Poisson transform therefore fulfills the semigroup property. Furthermore it holds that $P[f] >= 0$ for every $f >= 0$ due to the positivity of the kernel. Since the Poisson transform solves the Laplace equation, which is the diffusion equation with constant source term, it is an diffusion semigroup operator on $\mathbb{S}^2$. The maximum and minimum values of harmonic functions in $\mathbb{B}^2$ lie on the boundary $\mathbb{S}^2$. In addition it holds for a harmonic function that every function value at some $x \in \mathbb{B}^2$ is equal to the average over an arbitrary sphere around x in $\mathbb{B}^2$. It therefore generates no additional local extrema. These properties suggest the Poisson kernel as a smoothing filter. Figure 5.2 shows the Poisson transform at different scales on $\mathbb{S}^2$.

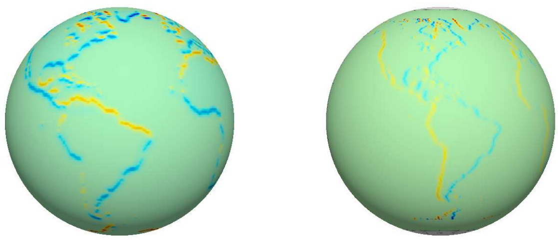

Figure 5.1: Outputs of the filters $\mathcal{R}(\rho)[\mathcal{Q}_r^{(1)}]$ and $\mathcal{R}(\rho)[\mathcal{Q}_r^{(1)}]$ at the scale $r = 0.99$.

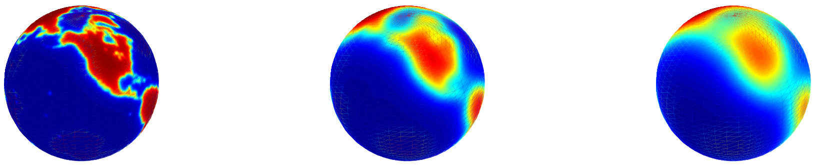

Figure 5.2: Top row: Poisson filtered images at decreasing scales

5.2 Plane wave analysis

We want to determine the orientation of a plane wave $a(t)e^{i\langle x,y\rangle}$ and the phase with respect the $\theta - \varphi$ plane in our local spherical coordinate system (see Figure 5.3). The direction of the plane wave is given by $y = [k \sin\alpha\cos\beta, k \sin\alpha\sin\beta,\ k \cos\alpha]^T$ where k is the frequency. $a(t)$ denotes the amplitude of the plane wave. Without loss of generality we can always choose the point ξ at which we evaluate the filter operations as the north pole $\xi = (\theta,\varphi) = (0,0)$. It is well known (see e.g. [1]) that a plane wave in $\mathbb{R}^3$ can be expanded in terms of spherical harmonics as

$$f(x) = a(t)e^{i\langle x,y\rangle} = a(t)\sum_{l\in\mathbb{N}}\sum_{m=-l}^{l}\hat{f}_{l,m}Y_{l,m}(\theta,\varphi) \tag{5.3}$$

with

$$\hat{f}_{l,m} = i^l j_l(rk)\overline{Y_{l,m}(\alpha,\beta)} \tag{5.4}$$

where $x = r\xi, y = k\omega$ and j_l is the spherical Bessel function of the first kind and order l. The expansion splits the plane wave into and angular part represented by the spherical harmonics and a part depending on the frequency of the wave described by the spherical Bessel function. Due to the nature of our filter kernels these act only on the *angular* portions of the plane wave. The frequency information k is encoded as the argument of the Bessel function is left untouched by our filter set. Using (4.9) and the property $D^l_{m,0} = (\frac{4\pi}{2l+1})^{1/2}\overline{Y_{l,m}}$ in conjunction with the Wigner-D function addition theorem [23]

$$\sum_{m=-l}^{l} D^l_{m,0}(\alpha,\beta,0)\overline{D^l_{m,1}(\theta,\varphi,0)} \tag{5.5}$$

$$= \overline{D^l_{0,1}(\alpha',\beta',0)} = D^l_{1,0}(\alpha,\beta,0) \tag{5.6}$$

the conjugate Poisson transforms of f, assuming that they are evaluated at the north pole, read

$$\mathcal{R}(\rho)[\mathcal{Q}_r^{(1)}] \star f = a(t) \sum_{l \in \mathbb{N}} \sum_{m=-l}^{l} r^l i^l j_l(rk) P_l^1(\cos\alpha)\cos\beta \tag{5.7}$$

$$\mathcal{R}(\rho)[\mathcal{Q}_r^{(2)}] \star f = a(t) \sum_{l \in \mathbb{N}} \sum_{m=-l}^{l} r^l i^l j_l(rk) P_l^1(\cos\alpha)\sin\beta \tag{5.8}$$

where P_l^m are the associated Legendre functions. The angle β is obtained as

$$\beta = \arctan \frac{R(\xi)[\mathcal{Q}_r^{(2)}] \star f}{R(\xi)[\mathcal{Q}_r^{(1)}] \star f}. \tag{5.9}$$

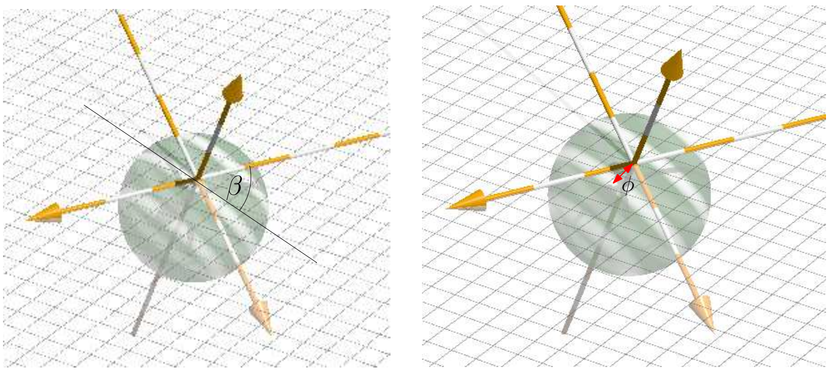

Figure 5.3: From left to right: Orientation angle β of the plane wave in the $\theta - \varphi$ plane with respect to the local coordinate system. Phase ϕ of the plane wave with respect to the local coordinate system.

Since

$$P_l^1(\cos\alpha) = -\sin\alpha \frac{d}{d\cos\alpha} P_l(\cos\alpha) \tag{5.10}$$

we notice that the bivector parts of the conjugate Poisson transform both act as differential operators with respect to $\cos\alpha$. We obtain the phase ϕ

$$\phi = \arctan \sqrt{\frac{(\mathcal{R}(0)[\mathcal{Q}_r^{(1)}] \star f)^2 + (\mathcal{R}(0)[\mathcal{Q}_r^{(2)}] \star f)^2}{(\mathcal{R}(0)[\mathcal{Q}_r^{(0)}] \star f)^2}} \tag{5.11}$$

Note that the determination of the orientation β and ϕ is invariant against the amplitude $a(t)$.

Figure 6.1 shows the filter outputs of the amplitude, the local orientation and the phase obtained by our filter set. It acts as the analogue to the classical Riesz transform in the plane which has been used to obtain local amplitude, orientation and phase of plane waves in $\mathbb{R}^2$.

6 Conclusion

We have given a spectral expression for the Hilbert transform on $\mathbb{S}^2$ in terms of spherical harmonic coefficients which provides an intuitive way of interpretation. The result was the important fact that the Hilbert transform on the sphere acts as a differential operator on the solution of the Poisson equation with boundary data on the sphere. It provides the partial derivatives with respect to the angles θ, φ. For functions which can be expanded into the product of a radial and an angular part, with frequency information encoded in the angular part, this results in differential operator without a high-pass characteristic. This justifies the transform as the spherical analogue of the Riesz transform where the partial derivatives in the Fourier domain of the Poisson equation solution are taken with respect to the Cartesian coordinates. The Hilbert transform on the sphere naturally arises from the Cauchy transform which defines a Poisson scale space in the unit ball. This might be treated as the counterpart in $\mathbb{R}^3$. It can be used for smoothing operations or singularity analysis for feature detection. Furthermore the orientation of plane waves arising in $\mathbb{R}^3_+$ can be analyzed providing a mechanism for orientation analysis on $\mathbb{S}^2$ without steering. Due to its derivative character, feature detectors in the plane based on derivatives might be transferred to the sphere to provide a robust feature detection adapted to the geometry of the sphere.
As we have seen we can use the Hilbert transform for taking derivatives with respect to the angles in the spherical harmonic domain. Using the integral formula (3.4), this differentiation can be carried out in the spatial domain without using the spherical harmonic transform on the sphere. A requirement is a proper sampling scheme on the sphere and a suitable quadrature formula. This turns out to be more stable than applying the operations in the spherical harmonic domain.

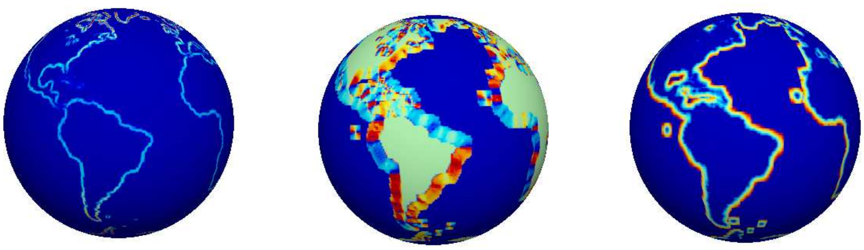

Figure 6.1: From left to right: Amplitude , orientation and phase output of the filters with a filter mask size of 9 pixels and a scale of $r = 0.99$.

Future work might include the derivation of higher order Hilbert transforms on $\mathbb{S}^2$ in order to analyze features provided by higher order derivatives. Furthermore it is desirable to obtain the instantaneous phase and amplitude of certain signals on the sphere and study singularities arising in the Poisson scale space for feature detection in an intensity invariant manner.

Bibliography

[1] William E. Baylis. *Electrodynamics: A Modern Geometric Approach (Progress in Mathematical Physics)*. Birkhäuser Boston, corrected edition, January 2004.

[2] S. Bernstein, R. Hielscher, and H. Schaeben. The generalized totally geodesic Radon transform and its application to texture analysis. *Mathematical Methods in the Applied Sciences*, 32(4), 2009.

[3] I. Bogdanova, X. Bresson, J. P. Thiran, and P. Vandergheynst. Scale space analysis and active contours for omnidirectional images. *Image Processing, IEEE Transactions on*, 16(7):1888–1901, 2007.

[4] Fred Brackx, Bram De Knock, and Hennie De Schepper. Generalized multidimensional Hilbert transforms in Clifford analysis. *International Journal of Mathematics and Mathematical Sciences*, 2006, 2006.

[5] Fred Brackx, Bram De Knock, Hennie De Schepper, and David Eelbode. On the interplay between the Hilbert transform and conjugate harmonic functions. *Mathematical Methods in the Applied Sciences*, 29(12):1435–1450, 2006.

[6] T. Bülow and G. Sommer. Hypercomplex signals - A novel extension of the analytic signal to the multidimensional case. *IEEE Transactions on Signal Processing*, 49(11):2844–2852, 2001.

[7] Philip Crotwell. Constructive approximation on the sphere. *Mathematical Geology*, 32(2):247–248, February 2000.

[8] R. Delanghe. On some properties of the Hilbert transform in Euclidean space. *Bull. Belg. Math. Soc. Simon Stevin*, 11(2):163–180, 2004.

[9] R. Delanghe, F. Sommen, and V. Soucek. *Clifford Algebra and Spinor-Valued Functions: A Function Theory for the Dirac Operator (Mathematics and Its Applications)*. Springer, 1 edition, April 1992.

[10] James R. Driscoll and Dennis M. Healy, Jr. Computing Fourier transforms and convolutions on the 2-sphere. *Adv. Appl. Math.*, 15(2):202–250, 1994.

[11] M. Felsberg and G. Sommer. The monogenic signal. *IEEE Transactions on Signal Processing*, 49(12):3136–3144, 2001.

[12] M. Felsberg and G. Sommer. The monogenic scale-space: A unifying approach to phase-based image processing in scale-space. *Journal of Mathematical Imaging and Vision*, 21(1):5–26, July 2004.

[13] W. Freeden, T. Gervens, and M. Schreiner. *Constructive approximation on the sphere*. Clarendon Press, Oxford, 1998.

[14] W. Freeden and K. Hesse. On the multiscale solution of satellite problems by use of locally supported kernel functions corresponding to equidistributed data on spherical orbits. *Studia Scientiarum Mathematicarum Hungarica*, 39(1):37–74, 2002.

[15] D. Gabor. Theory of communication. *Journal of the IEE (London)*, 93:429–457, 1946.

[16] V. Grau, H. Becher, and J.A. Noble. Phase-based registration of multi-view real-time three-dimensional echocardiographic sequences. *Lecture Notes in Computer Science*, 4190:612, 2006.

[17] Alan Jeffrey. *Table of Integrals, Series, and Products (Academic Press)*. Elsevier LTD, Oxford, 6. a. edition, August 2000.

[18] Ameesh Makadia, Lorenzo Sorgi, and Kostas Daniilidis. Rotation estimation from spherical images. In *ICPR '04: Proceedings of the Pattern Recognition, 17th International Conference on (ICPR'04) Volume 3*, pages 590–593, Washington, DC, USA, 2004. IEEE Computer Society.

[19] J.D. Mcewen, P. Vielva, Y. Wiaux, R.B. Barreiro, L. Cayon, M. P. Hobson, A. N. Lasenby, E. Martinez-Gonzalez, and J.L. Sanz. Cosmological applications of a wavelet analysis on the sphere. *Journal of Fourier Analysis and Applications*, 13(4):495–510, August 2007.

[20] M. Mellor and M. Brady. Phase mutual information as a similarity measure for registration. *Medical Image Analysis*, 9(4):330–343, 2005.

[21] ET Newman and R. Penrose. Note on the Bondi-Metzner-Sachs group. *Journal of Mathematical Physics*, 7:863, 1966.

[22] JC Nunes, S. Guyot, and E. Delechelle. Texture analysis based on local analysis of the bidimensional empirical mode decomposition. *Machine Vision and applications*, 16(3):177–188, 2005.

[23] David J. Pendleton. Euler angle geometry, helicity basis vectors, and the Wigner D-function addition theorem. *American Journal of Physics*, 71(12):1280–1291, 2003.

[24] N. Pugeault and N. Kruger. Multi–modal matching applied to stereo. In *Proceedings of the BMVC 2003*, pages 271–280, 2003.

[25] H. Schaeben. A unified view of methods to resolve the inverse problem of texture goniometry. *Textures and Microstructures*, 25(2):171–182, 1996.

[26] H. Schaeben and K.G. van den Boogaart. Spherical harmonics in texture analysis. *Tectonophysics*, 370(1-4):253–268, 2003.

[27] F. Sommen. Spherical monogenics on the Lie sphere. *J. Funct. Anal*, 92:372–402, 1990.

[28] Kasthuri Srinivasan, Hemant Mahawar, and Vivek Sarin. A multipole based treecode using spherical harmonics for potentials of the form r^{λ}. In *Computational Science - ICCS 2005*, volume 3514 of *Lecture Notes in Computer Science*, pages 107–114. Springer Berlin / Heidelberg, 2005.

[29] Elias M. Stein. *Singular Integrals and Differentiability Properties of Functions. (PMS-30).* Princeton University Press, February 1971.

[30] W.J. Thompson. *Angular momentum: an illustrated guide to rotational symmetries for physical systems*. Wiley-Interscience, 1994.

[31] Y. Wiaux, L. Jacques, P. Vielva, , and P. Vandergheynst. Fast directional correlation on the sphere with steerable filters. *The Astrophysical Journal*, 652(1):820–832, 2006.

[32] L. Wietzke and G. Sommer. The conformal monogenic signal. In *Pattern Recognition DAGM*, volume 5096 of *Lecture Notes in Computer Science*, pages 527–536. Springer Berlin / Heidelberg, 2008.